HAL
open science

Numerical convergence of a parameterisation method for the solution of a highly anisotropic two-dimensional elliptic problem.

Philippe Guillaume, Vladimir Latocha

To cite this version:

Philippe Guillaume, Vladimir Latocha. Numerical convergence of a parameterisation method for the solution of a highly anisotropic two-dimensional elliptic problem.. Journal of Scientific Computing, 2005, 25, pp.3, 423-444. hal-00092918

HAL Id: hal-00092918

https://hal.science/hal-00092918v1

Submitted on 12 Sep 2006

HAL is a multi-disciplinary open access archive for the deposit and dissemination of scientific research documents, whether they are published or not. The documents may come from teaching and research institutions in France or abroad, or from public or private research centers.

L'archive ouverte pluridisciplinaire **HAL**, est destinée au dépôt et à la diffusion de documents scientifiques de niveau recherche, publiés ou non, émanant des établissements d'enseignement et de recherche français ou étrangers, des laboratoires publics ou privés.

Numerical convergence of a parameterisation method for the solution of a highly anisotropic two-dimensional elliptic problem.

Philippe Guillaume[a] Vladimir Latocha[b]

[a] MIP, UMR 5640 (CNRS-UPS-INSA), INSA de Toulouse,
135 avenue de Rangueil, 31077 Toulouse Cedex 4, France
e-mail: Philippe.Guillaume@insa-toulouse.fr

[b] Institut Elie Cartan (UMR CNRS 7502)
Université Henri Poincaré - Nancy I
BP 239, 54506 Vandoeuvre-lès-Nancy Cedex, France
e-mail: latocha@iecn.u-nancy.fr

suggested running head: Parameterisation method for a highly anisotropic elliptic problem.

corresponding author: Vladimir Latocha. See above for mail and e-mail addresses. Phone number: +33 (0)3 83 68 45 65 Fax number: +33 (0)3 83 68 45 34

Abstract. *Highly anisotropic two-dimensional elliptic problems lead to severe numerical difficulties. In this paper, starting from a simple finite volume scheme, we present a parameterisation method that allows us to obtain the solution even if the anisotropy ratio is very large. We derive a formal asymptotic limit of the two dimensional anisotropic problem, in the case where the anisotropy ratio goes to infinity. This formal limit is used as a reference, and we show that the parameterisation method gives similar results, whereas the finite volume scheme fails to give an accurate solution. Numerical results are given, which indicate important parameters to be considered in order to obtain a good precision.*

Key words: anisotropic elliptic problems, finite volume methods, parameterisation methods, high anisotropy, ill-conditioned problems.

1 Introduction

Elliptic anisotropic problems arise in a wide range of problems; in plasma physics, semiconductor modelling, or porous media for instance. In studying these problems we must consider the discretization schemes as well as resolution algorithms for the obtained linear systems.

Let $\Omega =]0, L[\times]R_0, R_1[$ be a two dimensional domain, where $R_1 - R_0$ is of the same order as L. The four edges of the boundary of Ω are given by: $\partial\Omega_0 = \left\{(x,y) \in \overline{\Omega}, y = R_0\right\}$, $\partial\Omega_1 = \left\{(x,y) \in \overline{\Omega}, y = R_1\right\}$, $\partial\Omega_a = \left\{(x,y) \in \overline{\Omega}, x = 0\right\}$, $\partial\Omega_c = \left\{(x,y) \in \overline{\Omega}, x = L\right\}$. The problem that we study here was originally the determination of an electric field in a magnetized cavity, which explains the notation Ω_a and Ω_c since they were the anode and the cathode in the original problem.

On this domain we define a smooth vector field $B : (x,y) \in \overline{\Omega} \mapsto B(x,y) \in \mathbb{R}^2$. We assume that this field is non-zero in $\overline{\Omega}$. We denote by $\theta(x,y)$ the angle between $B(x,y)$ and the x axis, and $P(\theta(x,y))$ is the rotation matrix transforming the canonical basis (e_x, e_y) into the direct oriented orthonormal basis whose first vector is aligned with $B(x,y)$. The anisotropy of the problem is described by the conductivity matrix

$$\sigma(x,y) = \begin{bmatrix} \sigma_{xx} & \sigma_{xy} \\ \sigma_{xy} & \sigma_{yy} \end{bmatrix} = P(\theta(x,y)) \begin{bmatrix} \sigma_{\parallel}(x,y) & 0 \\ 0 & \sigma_{\perp}(x,y) \end{bmatrix} P(-\theta(x,y)), \tag{1}$$

and we propose to solve the equation with unknown W:

$$\begin{aligned} \nabla \cdot \mathcal{J}(x,y) &= S(x,y), \quad \forall (x,y) \in \Omega \\ \text{with } \mathcal{J}(x,y) &= -\sigma \, \nabla W(x,y), \end{aligned} \tag{2}$$

subject to the boundary conditions:

$$\begin{aligned} W(x,y) &= W_a(y)\,, \quad \forall (x,y) \in \partial\Omega_a \\ W(x,y) &= W_c(y)\,, \quad \forall (x,y) \in \partial\Omega_c \\ (\mathcal{J}(x,y)\cdot e_y) &= 0\,, \qquad \forall (x,y) \in \partial\Omega_0 \cup \partial\Omega_1\,, \end{aligned} \tag{3}$$

According to the definition (1), the principal directions of the conductivity matrix σ are aligned with the field and its orthogonal direction. When the field is along one of the basis vectors e_x or e_y, the conductivity matrix is diagonal in the basis (e_x, e_y), and the derivatives of the current $\frac{\partial}{\partial x} j(x,y)$ and $\frac{\partial}{\partial y} j(x,y)$ are proportional to $\frac{\partial}{\partial x} W(x,y)$ and $\frac{\partial}{\partial y} W(x,y)$ respectively. Hence, there will be no mixed derivatives $\frac{\partial^2 W}{\partial x \partial y}$ in the equation (2). If this situation happens for each point of Ω, then the techniques for discretizing one-dimensional problems can be easily extended [3, 16].

In the more general case where the eigenvectors are oblique, but of constant direction, it is possible to adapt the meshing in order to obtain precise schemes [20]. This situation even led to industrial codes in oil-reservoir simulations [1, 2]. The case where the direction of the anisotropy is (theoretically) arbitrary is studied in [5] and numerical tests are conducted only in the case where the anisotropy matrix is diagonal.

As for the solution of the linear system obtained after discretization, in most of the cases strongly anisotropic elliptic problems lead to linear systems that are out of reach of traditional iterative solvers. Specifically, the convergence is not always attained, and specialised preconditioners that can be considered to be close to multigrid methods are needed [8, 13]. More generally, multigrid methods seem to be a wise choice for solving such problems [5, 16].

We address the fairly general case where the direction of the anisotropy has smooth variations, but we assume that the *anisotropy ratio* $\gamma(x,y) = \frac{\sigma_\parallel(x,y)}{\sigma_\perp(x,y)}$ is constant over the whole domain, i.e. $\gamma(x,y) \equiv \overline{\gamma}$ (we shall relax this hypothesis in future work). Then the conductivity matrix reads:

$$\sigma(x,y) = P(\theta(x,y))\sigma_\perp(x,y) \begin{bmatrix} \overline{\gamma} & 0 \\ 0 & 1 \end{bmatrix} P(-\theta(x,y)).$$

Our aim is to solve (2) when it is highly anisotropic, that is for large $\overline{\gamma}$ (10^3 and more).

In the following, we do not use multigrid methods but we provide a method where direct solvers as well as traditional iterative solvers can be chosen for the linear system. This results in enlarging the range of applications of our code, since multigrid methods must be tailored in accordance with the problem to solve. As a starting point for the method we describe

in this paper, we choose a parameterisation of the highly anisotropic problem. This parameterisation then allows us to construct the solution of the highly anisotropic problem as a series. Adjusting proper values of the parameter, we can choose the situation where the coefficients of the series are solutions of isotropic problems, which are easy to solve numerically. Parameterisation methods succeeded to solve a broad range of problems, from waveguide propagation [10] to elasticity [11, 21], and we refer to [9] for an early work in this field.

In section 2.1, we describe a simple finite volume scheme that approximates an elliptic anisotropic problem in the general case. Then, in order to get a reference solution to the highly anisotropic problem, we let the anisotropy ratio go to infinity and we make a formal asymptotic analysis. This reduces the two dimensional problem to a one-dimensional diffusion equation. In section 3 we then proceed to present the main result of this paper, that is the use of a parameterisation method and the translation of the highly anisotropic problem into a sequence of easy-to-solve linear systems. Finally, we show numerical results in section 4.

We emphasize the fact that for the present problem, the result of the asymptotic analysis is sufficient to compute a good approximation of the solution. However, in future work we wish to compute the solution in the case where the anisotropy ratio is high in some parts of the domain, and of order one in other parts. Hence the present work is a first step in this direction.

2 Finite Volume Method and Reference Solution

2.1 Finite Volume Scheme

To discretize (2), we choose a cell centered finite volume scheme, and an even Cartesian grid. For sake of simplicity, we shall consider a grid which is regular in both directions. We define Δx to be the width of the control volumes, and Δy to be their height. The neighbours of the centre of the cell Ω_i are named as shown in figure 1. In the following, we only give the formulas that we chose in the construction of our finite volume scheme. A general description of the finite volume method and of the issues to be addressed can be found in [6].

Classically, we start from the integration of (2) on a control volume Ω_i.

Then we approximate

$$\begin{aligned}\int_{\Omega_i} \nabla \cdot \mathcal{J}\, dS &= \int_{\partial\Omega_i} \mathcal{J} \cdot n\, dl \\ &\approx \mathcal{J}_x^1\, \Delta y + \mathcal{J}_y^2\, \Delta x - \mathcal{J}_x^3\, \Delta y - \mathcal{J}_y^4\, \Delta x, \qquad (4)\end{aligned}$$

where $\mathcal{J}^k = \begin{pmatrix} \mathcal{J}_x^k \\ \mathcal{J}_y^k \end{pmatrix}$ is meant to approximate $\mathcal{J}$ at the midpoint of the edge k.

In order to provide an approximation of $\mathcal{J}^1$ for instance, we adopt $\left(\frac{\partial W}{\partial x}\right)^1 = \frac{W_E - W_C}{\Delta x} + \mathcal{O}(\Delta x^2)$, and $\left(\frac{\partial W}{\partial y}\right)^1 = \frac{W_N - W_S + W_{NE} - W_{SE}}{4\Delta y} + \mathcal{O}(\Delta x^2 + \Delta y^2)$. Eventually, taking $\mathcal{J}^1 = -\sigma^1 \left(\nabla W\right)^1$, with σ^1 being the arithmetic mean of σ at the points C and E (see figure 1), we obtain an expression of $\mathcal{J}^1$ involving data and unknowns W_i at the center of the control volumes. Adapting this procedure to the three other edges of the control volume, and inserting these formulæ in (4) leads to a finite volume scheme. We refer to [6] for further properties to be satisfied by finite volume schemes.

The boundary conditions are classically implemented by an appropriate meshing: the Neumann boundary coincides with edges of control volumes, and the Dirichlet boundary corresponds to centres of control volumes.

In the next subsection, we deal with the search of a numerical reference in order to validate or invalidate the solution obtained with our finite volume scheme.

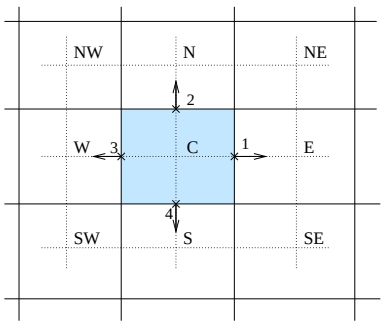

Figure 1: Notations for the neighbours of the centre of one cell.

2.2 Solution of the limit problem

One difficulty that arises in this study is the obtention of a reference. Indeed, what motivates our work is the lack of simple methods for solving

(2) when $\overline{\gamma}$ is large. More precisely, usual methods fail to provide a correct numerical solution when $\overline{\gamma}$ increases, and we showed in [14] that the finite-volume scheme of section 2.1 does not perform better.

In order to have a reference for large $\overline{\gamma}$, in this section we perform a formal asymptotic analysis of ((2),(3)) as $\overline{\gamma} \to \infty$. The main result of this section lies in proposition 1, where we show that this formal limit can be deduced from the solution of a one-dimensional diffusion problem. We postpone for future work the rigorous proof of convergence, but this formal limit can be used, as a first guess, to provide a reference for the parameterisation method we develop in section 3.

2.2.1 Natural coordinates, scaling

We rewrite here the problem in proper coordinates, and we scale the equations with respect to $\varepsilon = 1/\overline{\gamma} \to 0$. We propose a new coordinate system (α, β) such that $\nabla\alpha = \begin{pmatrix} B_y \\ -B_x \end{pmatrix}$ and $\nabla\beta = \begin{pmatrix} B_x \\ B_y \end{pmatrix}$, from which we define the orthonormal basis (which is actually a basis of eigenvectors of the conductivity matrix at a given point):

$$(e_\alpha, e_\beta) \quad = \quad \frac{1}{|B|}(\nabla\alpha, \nabla\beta). \tag{5}$$

Let us now define the coordinate change

$$\begin{aligned} f : U \subset \mathbb{R}^2 \quad &\to \quad V \supset \Omega \\ (\alpha, \beta) \quad &\mapsto \quad (x, y), \end{aligned}$$

and assume that it is continuously invertible (which depends on the shape and regularity of B). Then, the Jacobians of f and its inverse read:

$$J_f = \frac{1}{|B|^2} \begin{pmatrix} B_y & B_x \\ -B_x & B_y \end{pmatrix} \quad \text{and} \quad J_{f^{-1}} = \begin{pmatrix} B_y & -B_x \\ B_x & B_y \end{pmatrix}.$$

Thus, the metric of the new coordinate system reads $g_{ij} = 1/|B|^2\delta_{ij}$, which gives the following formulae for the gradient and the divergence operators:

$$\begin{aligned} \nabla f \quad &= \quad |B| \left(\partial_\alpha f \; e_\alpha + \partial_\beta f \; e_\beta\right) \\ \nabla \cdot F \quad &= \quad |B|^2 \left(\partial_\alpha \left(\frac{F_\alpha}{|B|}\right) + \partial_\beta \left(\frac{F_\beta}{|B|}\right)\right), \end{aligned}$$

where ∂_α (resp. ∂_β) stands for the derivative with respect to α (resp. β), and F_α (resp. F_β) stands for the component of F along e_α (resp. e_β). In these coordinates, the conductivity matrix is diagonal, and (2) reads:

$$-\partial_\alpha \left(\sigma_\perp \, \partial_\alpha W\right) - \partial_\beta \left(\sigma_\parallel \, \partial_\beta W\right) \quad = \quad \frac{1}{|B|^2} \, S(\alpha, \beta). \tag{6}$$

Furthermore, introducing the notation (n_α, n_β) to represent the coordinates of the unit vector normal to the boundary, the Neumann boundary condition (3) reads:

$$-n_\alpha\, \sigma_\perp\, \partial_\alpha W - n_\beta\, \sigma_\parallel\, \partial_\beta W \quad = \quad 0. \tag{7}$$

Finally, we want to analyze the problem when $\varepsilon = 1/\overline{\gamma} \to 0$. Assuming that all quantities are of order one, except $\sigma_\parallel = \overline{\gamma}\sigma_\perp = \frac{1}{\varepsilon}\sigma_\perp = \mathcal{O}(1/\varepsilon)$, then we are led to the following problem:

$$(\mathcal{P}_\varepsilon) \left\{ \begin{array}{rcll} -\partial_\alpha\,(\sigma_\perp\, \partial_\alpha W) - \frac{1}{\varepsilon}\partial_\beta\,(\sigma_\perp\, \partial_\beta W) & = & \frac{1}{|B|^2}\, S(\alpha,\beta) & \forall(\alpha,\beta)\in\Omega \\ W(\alpha,\beta) & = & W_a(y(\alpha,\beta))\,, & \forall(\alpha,\beta)\in\partial\Omega_a \\ W(\alpha,\beta) & = & W_c(y(\alpha,\beta))\,, & \forall(\alpha,\beta)\in\partial\Omega_c \\ -n_\alpha\, \sigma_\perp\, \partial_\alpha W - \frac{1}{\varepsilon}\, n_\beta\, \sigma_\perp\, \partial_\beta W & = & 0\,, & \forall(x,y)\in\partial\Omega_0\cup\partial\Omega_1. \end{array} \right. \tag{8}$$

This formulation is the basis for the formal asymptotic analysis.

2.2.2 Formal asymptotics

In order to obtain explicit results, we set the shape of the B field, whose field lines are given on figure 2. We now define some notation that will be useful for the derivation of the asymptotic model. The field lines being the curves $\alpha = k \in \mathbb{R}$, we denote by $\mathcal{C}(\alpha)$ the portion of curve $\overline{\Omega}\cap\{(\alpha,\beta), \beta\in\mathbb{R}\}$. We define α_c to be the value of α such that $\mathcal{C}(\alpha_c) = \partial\Omega_c$, and α_a is such that $\alpha \le \alpha_a \Rightarrow \mathcal{C}(\alpha)\cap\partial\Omega_a \neq \varnothing$. Finally, the extremities of $\mathcal{C}(\alpha)$ are denoted by $(\alpha, \beta_0(\alpha))$ and $(\alpha, \beta_1(\alpha))$.

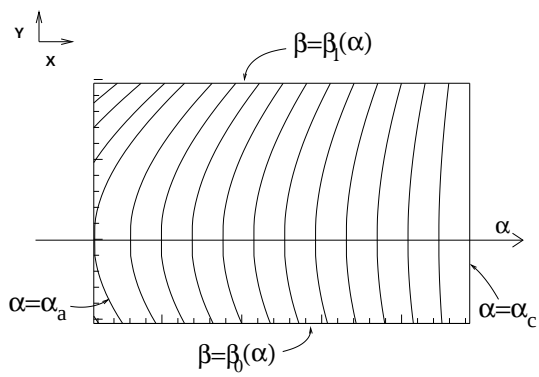

Figure 2: Field lines of B, and notation for the boundary.

We introduce the Hilbert expansion $W(\alpha,\beta) = W_0(\alpha,\beta) + \varepsilon\, W_1(\alpha,\beta) + \varepsilon^2\, W_2(\alpha,\beta) + \ldots$ into (8) and, identifying like powers of ε, we obtain the

following sequence of problems:

$$(P^0)\left\{\begin{array}{rcll} -\partial_\beta\left(\sigma_\perp\,\partial_\beta W_0\right) & = & 0 & \forall(\alpha,\beta)\in\Omega \\ W_0(\alpha,\beta) & = & W_a(y(\alpha,\beta))\,, & \forall(\alpha,\beta)\in\partial\Omega_a \\ W_0(\alpha,\beta) & = & W_c(y(\alpha,\beta))\,, & \forall(\alpha,\beta)\in\partial\Omega_c \\ n_\beta\,\sigma_\perp\,\partial_\beta W_0 & = & 0\,, & \forall(\alpha,\beta)\in\partial\Omega_0\cup\partial\Omega_1, \end{array}\right. \tag{9}$$

$$(P^1)\left\{\begin{array}{rcll} -\partial_\beta\left(\sigma_\perp\,\partial_\beta W_1\right) & = & \frac{1}{|B|^2}\,S+\partial_\alpha\left(\sigma_\perp\,\partial_\alpha W_0\right) & \forall(\alpha,\beta)\in\Omega \\ W_1(\alpha,\beta) & = & 0 & \forall(\alpha,\beta)\in\partial\Omega_a\cup\partial\Omega_c \\ \sigma_\perp\,\partial_\beta W_1 & = & -\frac{n_\alpha}{n_\beta}\sigma_\perp\,\partial_\alpha W_0, & \forall(\alpha,\beta)\in\partial\Omega_0\cup\partial\Omega_1, \end{array}\right. \tag{10}$$

and for $i>1$:

$$(P^i)\left\{\begin{array}{rcll} -\partial_\beta\left(\sigma_\perp\,\partial_\beta W_i\right) & = & \partial_\alpha\left(\sigma_\perp\,\partial_\alpha W_{i-1}\right) & \forall(\alpha,\beta)\in\Omega \\ W_i(\alpha,\beta) & = & 0 & \forall(\alpha,\beta)\in\partial\Omega_a\cup\partial\Omega_c \\ \sigma_\perp\,\partial_\beta W_i & = & -\frac{n_\alpha}{n_\beta}\sigma_\perp\,\partial_\alpha W_{i-1}, & \forall(\alpha,\beta)\in\partial\Omega_0\cup\partial\Omega_1. \end{array}\right. \tag{11}$$

Let us prove the following proposition, that gives properties of the formal limit $W_0(\alpha,\beta)$:

Proposition 1 If $W_a(y)\equiv w_a\in\mathbb{R}$, and $W_c(y)\equiv w_c\in\mathbb{R}$, then

(i) $\forall(\alpha,\beta)\in\Omega,\ \ \partial_\beta W_0=0$,

(ii) For $\alpha<\alpha_a,\ \ (\alpha,\beta)\in\Omega\Rightarrow W_0(\alpha)=w_a$,

(iii) For $\alpha_a\le\alpha\le\alpha_c$, $W_0(\alpha)$ is determined by the following one dimensional boundary value problem:

$$\left\{\begin{array}{rcl} -\dfrac{d}{d\alpha}\left(\mathbb{D}(\alpha)\dfrac{d}{d\alpha}W_0(\alpha)\right) & = & \displaystyle\int_{\beta_0(\alpha)}^{\beta_1(\alpha)}\frac{S(\alpha,\beta)}{|B(\alpha,\beta)|^2}\,d\beta \\ W_0(\alpha_a) & = & w_a \\ W_0(\alpha_c) & = & w_c, \end{array}\right. \tag{12}$$

where $\mathbb{D}(\alpha)=\int_{\beta_0(\alpha)}^{\beta_1(\alpha)}\sigma_\perp(\alpha,\beta)\,d\beta$.

Proof: Using the first equation of (9), then for fixed α we have $\sigma_\perp\partial_\beta W_0=k(\alpha)$, but since every $C(\alpha)$ crosses $\partial\Omega_0\cup\partial\Omega_1$, then $k(\alpha)\equiv 0$, which proves *(i)*. Hence, W_0 is a function of α only. For $\alpha<\alpha_c$, $C(\alpha)$ also crosses $\partial\Omega_a$, hence $W_0(\alpha)=w_a$ the value of the Dirichlet boundary condition. Finally, for $\alpha_a\le\alpha\le\alpha_c$, with reference to the identity $\int_{\beta_0(\alpha)}^{\beta_1(\alpha)}\partial_\beta\left(\sigma_\perp\,\partial_\beta W_1\right)\,d\beta=$

$\sigma_\perp \, \partial_\beta W_1|_{(\alpha,\beta_1(\alpha))} - \sigma_\perp \, \partial_\beta W_1|_{(\alpha,\beta_0(\alpha))}$, then defining

$$\begin{aligned} v_1(\alpha) &= \beta_1'(\alpha)\sigma_\perp(\alpha,\beta_1(\alpha)) - \beta_0'(\alpha)\sigma_\perp(\alpha,\beta_0(\alpha)) \\ v_2(\alpha) &= \left.\frac{n_\alpha}{n_\beta}\right|_{\beta_1(\alpha)} \sigma_\perp(\alpha,\beta_1(\alpha)) - \left.\frac{n_\alpha}{n_\beta}\right|_{\beta_0(\alpha)} \sigma_\perp(\alpha,\beta_0(\alpha)) \\ v(\alpha) &= v_1(\alpha) + v_2(\alpha), \end{aligned}$$

we get the following compatibility condition on the right-hand sides of (10), which is a drift-diffusion equation:

$$-\frac{d}{d\alpha}\left(\mathbb{D}(\alpha)\frac{d}{d\alpha}W_0(\alpha)\right) + v(\alpha)\frac{d}{d\alpha}W_0(\alpha) = \int_{\beta_0(\alpha)}^{\beta_1(\alpha)} \frac{S(\alpha,\beta)}{|B(\alpha,\beta)|^2}\, d\beta, \quad (13)$$

but one can prove that $v = v_1 + v_2 = 0$. If we focus on boundary $\partial\Omega_0$, we first consider it as a parametrized curve $\alpha \mapsto (\alpha, \beta_0(\alpha))$ in the (α,β) coordinates (we recall they are orthogonal). Then, the unit tangent vector has coordinates $k\,(1, \beta_0'(\alpha))$ with $k \in \mathbb{R}$, and n, the unit vector normal to the boundary, reads $k\,(\beta_0'(\alpha), -1)$. Hence the coordinates of n satisfy $\left.\frac{n_\alpha}{n_\beta}\right|_{\beta_0(\alpha)} = -\beta_0'(\alpha)$. Adapting this argument to $\partial\Omega_1$ leads to $v_1 + v_2 = 0$, which completes the proof of *(iii)*. □

We postpone for future work the rigorous proof of the convergence of the solution of (8) to W_0 defined by proposition 1, but we refer to Sili [19] for a rigorous proof in an analogous case. Indeed, with the exception of the transition in the vicinity of $\alpha = \alpha_a$, it is likely that our problem can be considered as the restriction to the linear case of the situation investigated in [19], where Sili obtains a general variational formulation that can be interpreted as the diffusion problem of proposition 1, together with error estimates. We also refer to [4] for numerous references about asymptotics of elliptic problems (among others) in thin domains, which lead to similar formulations as (8).

2.3 First numerical test

In this paragraph, we provide motivation for the parameterisation method by showing that our finite-volume scheme is clearly unable to provide a correct solution when the anisotropy ratio is large. The asymptotic solution given by proposition 1 is quite easy to compute numerically, the only difficulty being the implementation of the change of coordinates $f : (\alpha,\beta) \mapsto (x,y)$ and $f^{-1} : (x,y) \mapsto (\alpha,\beta)$ in order to take into account the spatial dependence of the coefficients of equation (2), which are given as functions of x and y. For sake of simplicity, we still denote the numerical solution to this problem by W_0. This solution is used as the reference for large $\overline{\gamma}$,

that is of order 10^3 and over, and we compare it to the solution computed by the finite-volume scheme W_{FV}. For $\overline{\gamma} = 10^4$ and $\overline{\gamma} = 10^6$, we plot the evolution of the relative l^∞ error $||W_0 - W_{FV}||_\infty / ||W_0||_\infty$ with respect to the number of nodes in both directions of the mesh (figure 3). We observe that for $\overline{\gamma} = 10^4$, one may expect fairly accurate results for refined meshes – though the memory requirements increase dramatically and may force the abandonment of direct methods for solving the linear system – but that for $\overline{\gamma} = 10^6$ the error is very high though the solution is theoretically closer to the reference, as figure 6 also illustrates. For practical applications [7], we wish to solve ((2),(3)) for ratios as high as 10^6, thus we improved this finite-volume scheme by the parameterisation method presented in next section.

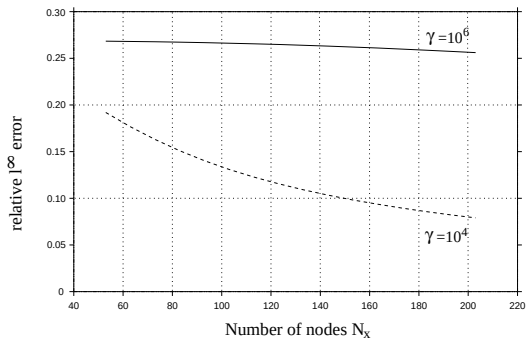

Figure 3: Relative l^∞ error between the asymptotic solution and the solution computed by the finite-volume scheme.

3 One parameterisation technique

In this section we follow ideas developed for instance by Guillaume and Masmoudi in the area of optimal shape design [9, 10], or more recently with Zeglaoui in the area of elasticity [11, 21]. In these works, the main idea is to make use of differential calculus in order to avoid too many calculations or too difficult calculations. To do so, one parametrizes the problem to be solved, and chooses a value of the parameter for which the problem is easy to solve. Next, one extrapolates the solution of the problem for different values of the parameter by constructing a series (one can think of a Taylor series).

The following provides another example of such a procedure. First, we shall define a parameterisation, and thence study the dependency of the

discretization of our problem on the parameter. We then define a series that approximates the solution of the elliptic problem for high anisotropy ratios, and we identify a sequence of problems whose solutions provide the coefficients of this series. We conclude this section by studying the convergence radius of the series, in order to prove that it can indeed be used to obtain the solution of the original problem.

3.1 Discretization

We present here the parameterisation of the anisotropic problem that allowed us to get round the numerical difficulties encountered by the finite-volume scheme. The method that we introduce also applies to other schemes under some linearity conditions that will be identified later on.

Let $\overline{\mathcal{T}}$ a mesh of Ω and $\mathcal{T} \subset \overline{\mathcal{T}}$ the part of the mesh that does not meet the boundary. We denote by $f_{\mathcal{T}} = (f_i)_{i \in \mathcal{T}}$ the vector of the values on each point of the mesh of a function f defined on $\mathbb{R}^2$. Hence, $W_{\mathcal{T}}$ is the vector $(W_i)_{i \in \mathcal{T}}$ which approximates $W(x, y)$ the solution of ((2),(3)), and $\sigma_{\mathcal{T}}$ is the vector of the conductivity matrix on each point of the mesh. The linear system discretizing ((2),(3)) reads:

$$A\, W_{\mathcal{T}} \quad = \quad b_{\mathcal{T}} - d_{\mathcal{T}}, \tag{14}$$

where A is the matrix of the linear system, obtained from (e.g.) the finite-volume scheme, $W_{\mathcal{T}}$ is the solution we seek, $b_{\mathcal{T}}$ takes into account the right-hand side of (2) and $-d_{\mathcal{T}}$ takes into account the Dirichlet condition.

To get around the numerical difficulties inherent in high anisotropy ratios, we are able to reduce the problem to a sequence of isotropic problems whose resolution, contrary to the highly anisotropic problem, is correct. To do so, we multiply $\sigma_\perp$ by a parameter ζ such that $\zeta\sigma_\perp \approx \sigma_\parallel$ (i.e. $\zeta \approx \overline{\gamma}$), and so define the conductivity matrix:

$$\tilde{\sigma}(\zeta; x, y) \quad = \quad P(\theta(x, y))\sigma_\perp(x, y) \begin{bmatrix} \overline{\gamma} & 0 \\ 0 & \zeta \end{bmatrix} P(-\theta(x, y)).$$

To this matrix we associate the problem $\mathcal{P}(\zeta)$, deduced from ((2),(3)) by replacing $\sigma(x, y)$ by $\tilde{\sigma}(\zeta; x, y)$. Hence $\mathcal{P}(1)$ is the original problem and $\mathcal{P}(\overline{\gamma})$ is an isotropic one. We then define the operators:

$$\begin{array}{lll} A: & \tilde{\sigma} & \mapsto (A_{ij})_{(i,j) \in \mathcal{T}^2} \\ d: & W_a, W_c, \tilde{\sigma} & \mapsto d_{\mathcal{T}} \end{array} \tag{15}$$

which leads to the more precise writing of $\mathcal{P}(\zeta)$:

$$A(\sigma(\zeta))\, W_{\mathcal{T}} \quad = \quad b_{\mathcal{T}} - d_{\mathcal{T}}(W_a, W_c, \sigma(\zeta)), \tag{16}$$

where tilde symbols were omitted for sake of clarity.

Viewing equation (15) as a problem dependent on the single parameter ζ, our goal is the construction of an approximation of the sum

$$W_N(\zeta; x, y) \quad = \quad \sum_{k=0}^{N} W^{(k)}(\zeta_0; x, y) \, \frac{(\zeta - \zeta_0)^k}{k!}. \tag{17}$$

We adopt the following hypotheses, which hold for a large class of schemes discretizing ((2),(3)), and which obviously hold for the scheme introduced in section 2.1:

Hypothesis 1 Let A and d be defined by (15). We suppose that $\sigma \mapsto A(\sigma)$ and $\sigma \mapsto d(W_a, W_c, \sigma)$ are linear.

From these hypotheses, it is easy to deduce the following proposition.

Proposition 2 If $W_{\mathcal{T}}$ can be expanded in powers of $(\zeta - \zeta_0)$ as

$$W_{\mathcal{T}}(\zeta) \quad = \quad \sum_{k=0}^{+\infty} W_{\mathcal{T}}^{(k)}(\zeta_0) \, \frac{(\zeta - \zeta_0)^k}{k!},$$

then the vectors $W_{k,\mathcal{T}} = \frac{W_{\mathcal{T}}^{(k)}(\zeta_0)}{k!}$ are solutions of:

$$\begin{aligned} A(\sigma(\zeta_0)) \, W_{0,\mathcal{T}} &= b_{\mathcal{T}} - d_{\mathcal{T}}(W_a, W_c, \sigma(\zeta_0)) \\ A(\sigma(\zeta_0)) \, W_{1,\mathcal{T}} &= -A(D\sigma) \, W_{0,\mathcal{T}} - d_{\mathcal{T}}(W_a, W_c, D\sigma) \\ A(\sigma(\zeta_0)) \, W_{k,\mathcal{T}} &= -A(D\sigma) \, W_{k-1,\mathcal{T}} \qquad k \geq 2, \end{aligned} \tag{18}$$

where $D\sigma = P(\theta(x,y)) \begin{bmatrix} 0 & 0 \\ 0 & \sigma_\perp(x,y) \end{bmatrix} P(-\theta(x,y))$.

Proof: Let us substitute $W_{\mathcal{T}}(\zeta) = \sum_{k=0}^{+\infty} W_{\mathcal{T}}^{(k)}(\zeta_0) \, \frac{(\zeta-\zeta_0)^k}{k!}$ and $\sigma(\zeta) = \sigma(\zeta_0) + D\sigma \cdot (\zeta - \zeta_0)$ into equation (16). Using the linearity of A and d with respect to σ and gathering like powers of $(\zeta - \zeta_0)^k$, the proposition follows. $\square$

Supposing that the hypotheses of proposition 2 hold, let us describe the computation of the first N terms of the expansion in powers of $(\zeta - \zeta_0)$:

$$\mathcal{W}_{N,\mathcal{T}}(\zeta) \quad = \quad \sum_{k=0}^{N} W_{k,\mathcal{T}} \, (\zeta - \zeta_0)^k, \tag{19}$$

with $\{W_{k,\mathcal{T}}, k = 0, \ldots, N\}$ the solutions of linear systems (18). System

$$A(\sigma(\zeta_0)) \, W_{0,\mathcal{T}} \quad = \quad b_{\mathcal{T}} - d_{\mathcal{T}}(W_a, W_c, \sigma(\zeta_0))$$

shows no essential difference from the system encountered in the preceding section, $A(\sigma(\zeta_0))$ simply discretizes an isotropic elliptic problem. Hence we can use the resolution already implemented. Once $W_{0,\mathcal{T}}$ is known, we evaluate its matrix-vector product with $A(D\sigma(\zeta_0))$ and we determine the right-hand side:

$$A(\sigma(\zeta_0))\, W_{1,\mathcal{T}} \quad = \quad -A(D\sigma(\zeta_0))\, W_{0,\mathcal{T}} - d_{\mathcal{T}}(W_a, W_c, D\sigma(\zeta_0)).$$

This procedure is then iterated for the computation of all $\{W_{k,\mathcal{T}}, k \geq 2\}$:

$$A(\sigma(\zeta_0))\, W_{k,\mathcal{T}} \quad = \quad -A(D\sigma(\zeta_0))\, W_{k-1,\mathcal{T}}.$$

We remark that $A(\sigma(\zeta_0))$ is the matrix for every system, and our use of a direct solver is an advantage here since the factorization can be used from the second system onwards. In the case of large linear systems, the time spent for the factorization is much larger than the time needed to compute the solution once the factorization is known, so the computation of the coefficients of the expansion are relatively inexpensive.

3.2 Convergence of the series

At $\zeta = 1$, the problem we must solve is the original problem, it is highly anisotropic if $\overline{\gamma} \gg 1$. At $\zeta_0 = \overline{\gamma}$, the problem is isotropic, and we recover the solution at $\zeta = 1$ from the Taylor expansion computed at the point $\zeta_0 = \overline{\gamma}$ (see equation (19)).

However, we are yet to prove that this series converges. This proof is easy for the continuous problem. Specifically, if we replace σ by $\sigma(\zeta)$ in ((2), (3)), we must find the parameterised solution $W(\zeta)$. The variational formulation of this problem leads us to search for $\widehat{W} \in H_0^1(\Omega)$ such that

$$\forall v \in H_0^1(\Omega), \qquad a(\sigma(\zeta); \widehat{W}(\zeta), v) \quad = \quad l(v) - a(\sigma(\zeta); W_D, v), \quad (20)$$

where $W_D \in H^1(\Omega)$ is a function that satisfies the inhomogeneous Dirichlet boundary conditions, $a(\sigma(\zeta); W, v) = \int_\Omega \sigma(\zeta) \nabla W \circ \nabla v \, dx\, dy$ and $l(v) = \int_\Omega S \cdot v \, dx\, dy$. The weak solution $W(\zeta) \in H^1(\Omega)$ is then given by $W = \widehat{W} + W_D$ [12].

We are then in a position to prove the following proposition:

Proposition 3 Let $\widehat{W}(\zeta)$ be the solution to (20). Then $\zeta \mapsto \widehat{W}(\zeta)$ is analytical on the half space $\{\zeta \in \mathbb{C}, Re\ \zeta > 0\}$.

Proof: The variational problem admits a solution (with analytical dependence on the data) for all $\zeta \in \mathbb{C}$ such that $Re\ \zeta > 0$ [15]. The proposition follows (see [11] for detailed arguments). □

A straightforward consequence of proposition 3 is the following corollary (see figure 4 for graphical representation of the convergence radius):

Corollary 1 For $\zeta_0 > 0$, $W(\zeta)$ can be expanded into a power series around ζ_0:

$$W(\zeta; x, y) \quad = \quad \sum_{k=0}^{+\infty} w_k(x, y)\ (\zeta - \zeta_0)^k, \tag{21}$$

with $w_k \in H_0^1(\Omega)$ for $i \geq 1$. This series converges at least for $|\zeta - \zeta_0| < \zeta_0$, hence for $\zeta_0 > 1$ the series converges at $\zeta = 1$ to the solution of ((2),(3)).

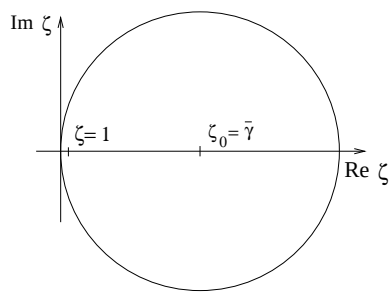

Figure 4: Convergence disk of the series in the continuous case.

Remark 1 Defining $a_0(W, v) = a(\sigma(\zeta_0), W, v)$ and $a'(W, v) = a(D\sigma, w, v)$ (we recall that $D\sigma$ is defined in proposition 2), then it is easy to show that the coefficients of (21) satisfy the following sequence of problems, whose solutions are sought in $H_0^1(\Omega)$:

$$\begin{array}{lll} \forall v \in H_0^1(\Omega), & a_0(\widehat{w}_0, v) & = \quad l(v) - a_0(W_D, v) \\ \forall v \in H_0^1(\Omega), & a_0(w_1, v) & = \quad -a'(w_0, v) - a'(W_D, v) \\ \forall v \in H_0^1(\Omega), & a_0(w_i, v) & = \quad -a'(w_{i-1}, v) \qquad i \geq 2, \end{array}$$

where $w_0 = \widehat{w}_0 + W_D$. It is interesting to compare this sequence to the one given in proposition 2.

Corollary 1 shows that the series (21) can be used to approximate the solution of the highly anisotropic problem ((2),(3)). However, we are dealing here with the continuous case and things can differ slightly when instead considering the sequence of discretized problems of proposition 2. In the next section, we shall see that the series (19) (discrete case) provides a good approximation for $W(1)$, that is for the solution to ((2),(3)), yet we will observe that the number of terms to be summed should be carefully chosen. We refer to [11] for a similar phenomenon.

4 Numerical results

In this section we present some results about the numerical convergence of the series constructed from proposition 2. In the following, we choose a right-hand side which is typical in plasma physics applications [14]. This choice indeed leads to a right-hand side of order 1 in the adimensional equation (8).

We first define some notation. Then we describe a change of variables that is necessary for sake of numerical precision. Eventually, we present some numerical results.

4.1 Notation

We recall that, for sake of simplicity, the numerical solution given by proposition 1 is also denoted by W_0. We emphasize the fact that there is a discretization error in $W_0(\alpha)$ as well as an interpolation error when constructing $W_0(x(\alpha,\beta), y(\alpha,\beta))$ (see section 2.2.1). This will result in some numerical noise on the error when taking W_0 as a reference.

We propose the following notation:

- M_x denotes the number of nodes of the mesh in the x direction. In computations, we always used $M_x \times M_x$ meshes.
- e_N is defined by $e_N = \| \mathcal{W}_{N,\mathcal{T}} - W_0 \|_{l^\infty} \; / \; \| W_0 \|_{l^\infty}$, where the functions are compared at the mesh points. We recall that $\mathcal{W}_{N,\mathcal{T}}$ is given by (19).
- We shall see that for fixed M_x and γ, e_N has a minimum with respect to N. We denote by N_{opt} the value of N where the minimum is reached, and $e_{N_{opt}}$ the value of this minimum.

4.2 Change of variables

Following the result of proposition 2, we have to sum:

$$\mathcal{W}_{N,\mathcal{T}}(\zeta) \quad = \quad \sum_{k=0}^{N} W_{k,\mathcal{T}} \, (\zeta - \zeta_0)^k .$$

For our purpose, we choose $\zeta = \overline{\gamma}$ and $\zeta_0 = 1$, and the series reads $\mathcal{W}_{N,\mathcal{T}}(\zeta) = \sum_{k=0}^{N} W_{k,\mathcal{T}} \; (\overline{\gamma} - 1)^k$ so that for $\overline{\gamma} = 10^6$ for instance, the factor $(\overline{\gamma} - 1)^k$ rapidly reaches large values. Since we expect the term $W_{k,\mathcal{T}} \; (\overline{\gamma} - 1)^k$ to be converging to zero, we should at least expect it is of order 1, hence $W_{k,\mathcal{T}}$ is smaller than $(\overline{\gamma} - 1)^{-k}$. As a result, after some iterations, it becomes smaller than the smallest floating point number that can be represented in standard representations, and it is numerically zero.

In order to avoid dividing and multiplying by large numbers, we adopt the new unknowns $\widetilde{W}_{k,\mathcal{T}} = W_{k,\mathcal{T}}\ (\zeta - \zeta_0)^k$. It is easy to show that they satisfy the sequence of linear systems:

$$\begin{aligned}
A(\sigma(\zeta_0))\ \widetilde{W}_{0,\mathcal{T}} &= b_{\mathcal{T}} - d_{\mathcal{T}}(W_a, W_c, \sigma(\zeta_0)) \\
A(\sigma(\zeta_0))\ \widetilde{W}_{1,\mathcal{T}} &= \Big(-A(D\sigma)\ \widetilde{W}_{0,\mathcal{T}} - d_{\mathcal{T}}(W_a, W_c, D\sigma)\Big) \cdot (\zeta - \zeta_0) \\
A(\sigma(\zeta_0))\ \widetilde{W}_{k,\mathcal{T}} &= \Big(-A(D\sigma)\ \widetilde{W}_{k-1,\mathcal{T}}\Big) \cdot (\zeta - \zeta_0) \qquad k \geq 2,
\end{aligned}$$

and we are led to computing $\mathcal{W}_{N,\mathcal{T}}(\zeta) = \sum_{k=0}^{N} \widetilde{W}_{k,\mathcal{T}}$. Figure 5 provides an example of the improvement due to this change, and also illustrates the existence of the numerical horizon after $N = 53$. Though the difference between the solutions obtained with one set of unknowns or the other is small, the change of unknowns allows us to study the convergence of the error with respect to N.

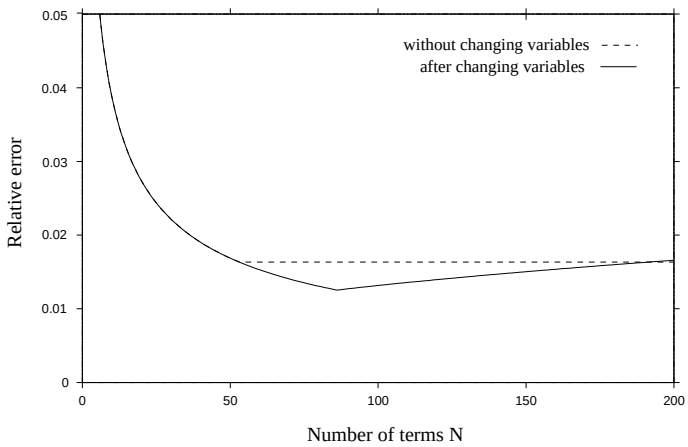

Figure 5: For $M_x = 200$ and $\overline{\gamma} = 10^6$, we plot e_N with respect to N. Without changing unknowns, the coefficient $W_{k,\mathcal{T}}$ is numerically zero after $k = 53$ and the evolution of the series stops, which does not happen with the equivalent set of unknowns $\widetilde{W}_{k,\mathcal{T}}$.

4.3 Analysis of the results

Before evaluating the influence of M_x, $\overline{\gamma}$ and N on the error e_N, we compare the results obtained by the finite volume scheme, by the parameterisation method, and the reference asymptotic solution. For $\overline{\gamma} = 10^6$, we arbitrarily

choose $M_x = 200$ and $N = 50$. We plot the results with respect to α, since we expect the solution of ((2),(3)) not to depend on β for large $\overline{\gamma}$ (see proposition 1). Figure 6 shows that the results obtained by the parameterisation method are close to the reference solution, whereas the finite volume scheme leads to a large discrepancy.

These results are already satisfactory. However, we must still investigate the effect of the numerical parameters M_x and N on the error; this is the object of the following.

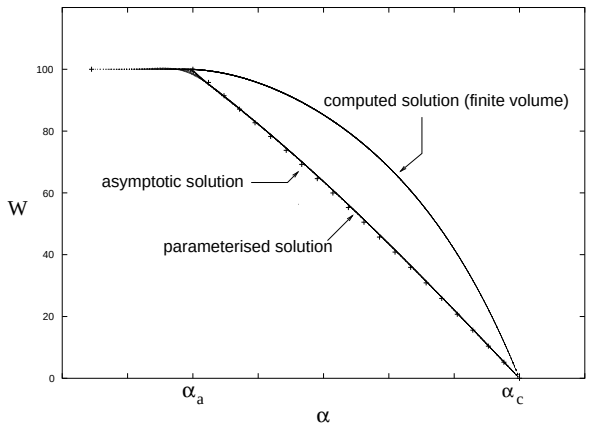

Figure 6: For $\overline{\gamma} = 10^6$, $M_x = 200$ and $N = 50$, comparison between the reference asymptotic solution W_0, the solution computed through the finite volume scheme, and the solution obtained following proposition 2.

4.3.1 Existence of an optimal number of terms

If we look at figure 5, we see that the series does not converge. Instead, there is an optimal numbers of terms (around 80 in this case) where the error is minimal. It is clear that the discrete problem does not behave exactly like the continuous one. In our case, just like in [11], though we were able to prove the convergence of the series in the continuous case, the convergence may be difficult to obtain in the discrete case, especially close to the boundary of the convergence disk $|\zeta - \zeta_0| < \zeta_0$. This is indeed the case when we want to extrapolate the solution at $\zeta = 1$ with $\zeta_0 \gg 1$.

This phenomenon has already been observed in [11], and it was proved that the optimal number of terms behaves like $log(1/h)$ where h is the mesh size. Furthermore, it was showed that the series with coefficients computed in the discrete case, truncated after the optimal number of terms, converges

to the limit of the continuous series. As for the present elliptic problem, we cannot make as precise an analysis because we lack information concerning the convergence of the numerical scheme. Nevertheless, we shall verify that we observe the same properties.

4.3.2 Evolution of the error with respect to the mesh size

For the following tests, we choose $\overline{\gamma} = 10^6$ in order to be close to the reference solution and to demonstrate the robustness of the method. We then study the influence of M_x on the truncated series e_N.

For fixed M_x, we locate N_{opt} and store $e_{N_{opt}}$. Figure 7 shows the evolution of these quantities with respect to M_x. As in [11], N_{opt} seems to behave like $a\ log(M_x) + b$ (fitting by least squares gives $a \simeq 70$ and $b \simeq 33$), hence the increase of N_{opt} with M_x is slow. Moreover, $e_{N_{opt}}$ seems to converge when the mesh size tends to zero, but the convergence is also slow.

Comparing the error $e_{N_{opt}}$ for, say, $M_x = 50$ and $M_x = 290$, one may think that the former is a good choice for practical computations since it leads to almost the same precision though it requires much less time. Indeed, N_{opt} (that is the number of terms we have to compute) is smaller, and the size of the linear systems that must be solved is also smaller. Yet, figure 8 shows that if M_x is small, then not knowing precisely N_{opt} leads to much less precision on the solution. In fact, the results of figure 7 do not give N_{opt} in the general case, and its determination is not straightforward in practice. Hence $M_x = 290$ is a much safer choice. The choice of N_{opt} is discussed in [11], and will be an important issue in the development of the present work.

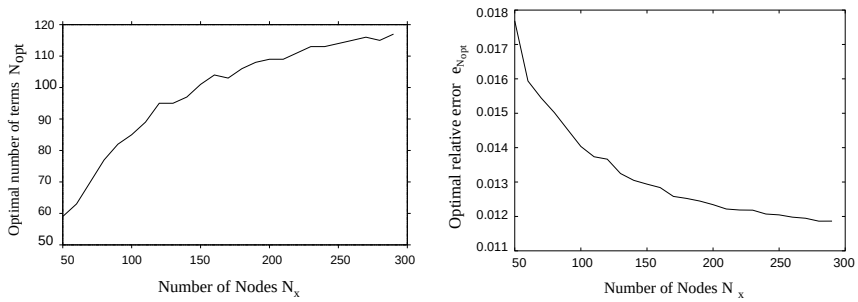

Figure 7: Evolution of N_{opt} and $e_{N_{opt}}$ with respect to M_x.

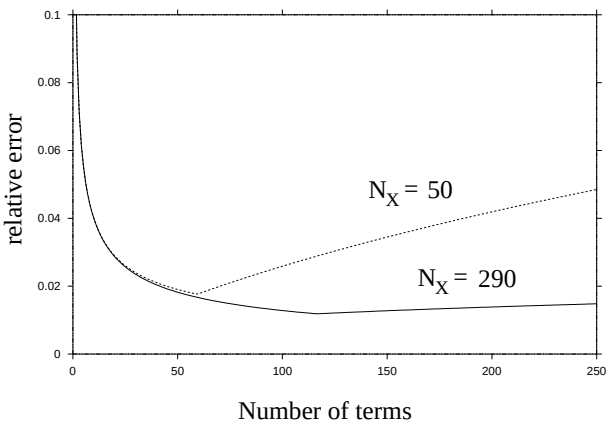

Figure 8: Evolution of the error with respect to N, for $M_x = 50$ and $M_x = 290$.

4.3.3 Evolution of N_{opt} with respect to $\overline{\gamma}$

We recall that the reference solution W_0 is assumed to be the limit of (8) as $\overline{\gamma} \to \infty$. Hence, for fixed M_x, we do not expect the error e_N to be small when $\overline{\gamma}$ is not large. For instance, taking $M_x = 290$, we find $e_{N_{opt}} \simeq 24 \cdot 10^{-2}$ for $\overline{\gamma} = 1$ and $e_{N_{opt}} \simeq 7 \cdot 10^{-2}$ for $\overline{\gamma} = 10$. This encourages us to focus on the interval $\overline{\gamma} \in [10^2,\ 10^7]$, and to be cautious when analyzing the error for $\overline{\gamma} < 10^4$.

On figure 9 we plot the evolution of e_N with respect to N and $\overline{\gamma}$. Moreover, we focus on the variation of the error between 10^{-2} and $2 \cdot 10^{-2}$ in order to learn more about the behaviour of N_{opt}. We observe that N_{opt} appears to be independent of $\overline{\gamma}$ for $\overline{\gamma} > 10^5$. What is more surprising is that N_{opt} becomes large for $\overline{\gamma} \simeq 10^3$, and e_N reaches *smaller* values in this case. In other words, the series has better convergence for $\overline{\gamma} \simeq 10^3$.

There are several factors which may help to explain this phenomenon: we saw that since $\zeta = 1$ is close to the boundary of the convergence disk of the series (21) (continuous case), the convergence of the series in the discrete case is difficult or not attained at all. If $\zeta_0 = \overline{\gamma}$ is not very large, $\zeta = 1$ is relatively far from the boundary and we can expect the convergence in the discrete case (see figure 4). On the other hand, the reference is no longer valid for $\overline{\gamma}$ of order 1, and the error should increase as $\overline{\gamma}$ decreases. These arguments could be the explanation for the better behaviour of e_N for intermediate values of $\overline{\gamma}$: that is it should be large enough to agree with the reference solution, and small enough to have better convergence properties.

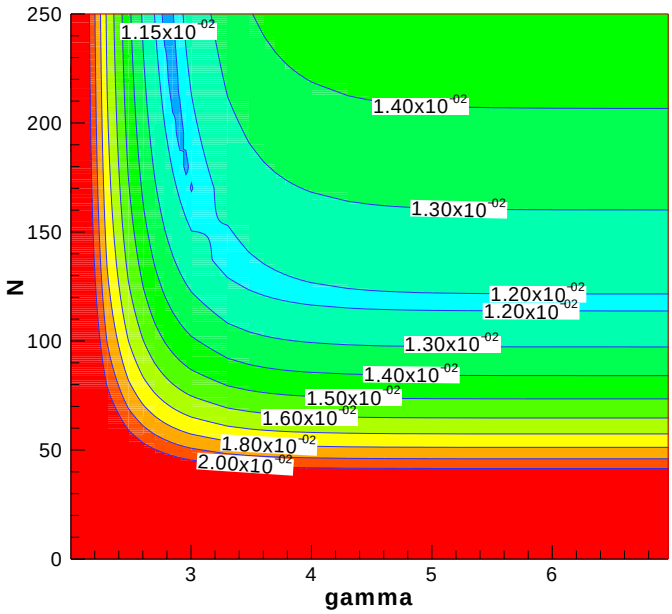

Figure 9: For a 290x290 mesh, evolution of the error with respect to $\log_{10} \overline{\gamma}$ and N the number of terms of the series.

5 Conclusion

In this paper we have devised a method for computing the solution of an anisotropic problem. We developed a parametrization method, which is based on constructiong a series whose coefficients are solutions of problems that are easy to solve numerically. Thus it can use classical discretization schemes and classical linear system solvers as a basis. This method allowed us to find a good approximation of the solution of ((2),(3)) even when the anisotropy ratio is as high as 10^7. We proved convergence of the series in the continuous case, but we observed that the situation is slightly different when instead considering the discretized problems. More precisely, the best approximations are obtained when summing a finite number of terms, N_{opt}, of the series. We showed that N_{opt} depends on the size of the mesh, that it seems to behave as $\log(1/M_x)$, but that it is independent of $\overline{\gamma}$ when the latter is large. In practical computations, one would need to know N_{opt}, but we showed that refined meshes lead not only to a smaller error, but also to a smaller variation of the error with respect to the number of summed terms. In other words, fine meshes can compensate for a lack of precise knowledge of N_{opt}. However, we intend to pursue further studies which will address the determination of N_{opt} without comparing the computed solution to a reference.

Acknowledgements: Part of this work was supported by the Japanese Society for the Promotion of Science. Vladimir Latocha also wishes to thank professor Kazuo Aoki, from the department of Aeronautics and Astronautics of Kyoto University, for his kind welcome shown to this author during his postdoctoral studies.

References

[1] R. Ababou (1991). *Approaches to large scale unsaturated flow in heterogeneous, stratified, and fractured geologic media*, U.S. Nuclear Regulatory commission report, NUREG/CR-5473

[2] R. Ababou, L.W.Gelhar, C.Hempel (1992). Serial and parallel performance on large matrix systems, *Cray channels*

[3] F.Brezzi, L.D.Marini, P.Pietra (1988). Numerical Simulation of semiconductor devices, *Istituto di analisi numerica, pubblicazioni n.608*

[4] P.G. Ciarlet (1997). *Mathematical Elasticity, vol. II: theory of plates*, North Holland

[5] P.I.Crumpton, G.J.Shaw, A.F.Ware (1995). Discretisation and multigrid solution of elliptic equations with mixed derivative terms and strongly discontinuous coefficients, *J. Comput. Phys.* **166**, 343-358

[6] R.Eymard, T.Gallouët, R.Herbin (2000). Finite volume methods, in P.G.Ciarlet, J.L.Lions (eds.), *Handbook of numerical analysis, vol VII*, North Holland, pp 713-1020

[7] L. Garrigues (1998). *Modélisation d'un propulseur à plasma stationnaire pour satellites*, thèse de doctorat de l'université Paul Sabatier, Toulouse (France)

[8] L. Giraud, R.S.Tuminaro (1999). Schur complement preconditioners for anisotropic problems, *IMA J. Numer. Anal.* **19**, 1-18

[9] Ph. Guillaume, M. Masmoudi (1994). Computation of high order derivatives in optimal shape design, *Numer. Math.* **67** no. 2, 231-250

[10] Ph. Guillaume, M. Masmoudi (1997). Solution to the time-harmonic Maxwell's equations in a waveguide, use of higher order derivatives for solving the discrete problem, *SIAM J. Numer. Anal.* **34** no.4, 1306-1330

[11] Ph. Guillaume, M. Masmoudi, A. Zeglaoui (2002). From compressible to incompressible materials via an asymptotic expansion, *Numer. Math.*, **91** no. 4, 649-673

[12] W. Hackbusch (1992). *Elliptic Differential Equations, theory and numerical treatment*, Springer Verlag

[13] B.N.Khoromskij, G.Wittum (1999). Robust Schur complement method for strongly anisotropic elliptic equations, *Numer. Linear Algebra Appl.*, **6**, 621-653

[14] V. Latocha (2001). *Deux problèmes en transport des particules chargées intervenant dans la modélisation d'un propulseur ionique*, thèse de doctorat de l'INSA Toulouse, INSA de Toulouse (France)

[15] J.L. Lions, E. Magenes (1968). *Problèmes aux limites non homogènes et applications*, Dunod

[16] J. Molenaar (1995). Adaptive multigrid applied to a bipolar transistor problem, *Appl. Numer. Math.* **17** no.1, 61-83

[17] A. Nayfeh (1973). *Perturbation methods*, Wiley-interscience

[18] S.Selberherr (1984). *Analysis and simulation of semiconductor devices*, Springer Verlag

[19] A. Sili (1999). Asymptotic behaviour of the solutions of monotone problems in flat cylinders, *Asympt. Anal.* **19** no. 1, 19-33

[20] D. Thangaraj, A. Nathan (1998). A rotated monotone difference scheme for the two dimensional anisotropic drift diffusion equation, *J. Comput. Phys.* **145** 445-461

[21] A. Zeglaoui (2000). *Approximation de problèmes singuliers par un développement asymptotique*, thèse de doctorat, INSA de Toulouse (France)